

Removing Distortion Effects in Music Using Deep Neural Networks

Johannes Imort*, Giorgio Fabbro[†], Marco A. Martínez Ramírez[‡],
Stefan Uhlich[†], Yuichiro Koyama[‡], and Yuki Mitsufuji[‡]

*RWTH Aachen University, [†]Sony Europe B.V., Stuttgart, Germany, [‡]Sony Group Corporation, Tokyo, Japan

Abstract—Audio effects are an essential element in the context of music production, and therefore, modeling analog audio effects has been extensively researched for decades using system-identification methods, circuit simulation, and recently, deep learning. However, only few works tackled the reconstruction of signals that were processed using an audio effect unit. Given the recent advances in music source separation and automatic mixing, the removal of audio effects could facilitate an automatic remixing system. This paper focuses on removing distortion and clipping applied to guitar tracks for music production while presenting a comparative investigation of different deep neural network (DNN) architectures on this task. We achieve exceptionally good results in distortion removal using DNNs for effects that superimpose the clean signal to the distorted signal, while the task is more challenging if the clean signal is not superimposed. Nevertheless, in the latter case, the neural models under evaluation surpass one state-of-the-art declipping system in terms of source-to-distortion ratio, leading to better quality and faster inference.

Index Terms—Audio effect removal, distortion removal, declipping.

I. INTRODUCTION

WITH the emergence of musical recordings, audio effects have become an indispensable tool in the music production process. They are used by musicians as a creative device to alter the sound characteristics of their instruments, and by sound engineers to craft a balanced mix from multiple recording tracks [1].

Generally, there is a wide variety of different audio effects: non-linear audio effects apply a non-linear function to the signal either with short (*e.g.*, distortion) or long temporal dependencies (*e.g.*, compressor). Modulation-based effects are time-varying and alter the audio signal based on a low-frequency modulation signal (*e.g.*, chorus). Other noteworthy effects based on time are delay and artificial reverberation. Lastly, filter-based audio effects alter the frequency spectrum of the signal (*e.g.*, equalizer) and can also be time-varying (*e.g.*, wah-wah) [2].

For the task of mixing and automatic remixing [3], the dry (*i.e.* unprocessed) source tracks are required. Given the recent advances in automatic mixing [4, 5] and music source separation [6], a system could be developed that facilitates

the adjustment of a stereo mixture to the user’s taste and preferences similar to [7]. However, today’s source separation systems are commonly trained on data that is based on music stems (*e.g.*, MUSDB18 [8]). Usually, a stem is mixed by a sound engineer from a group of processed audio tracks that belong together (*e.g.*, all drum microphone tracks) using audio effects [9]. Thus, separating sources with a system trained on stems does not consider the mixing process, and, hence, the output of such a system contains the wet (*i.e.* processed) signal. Additionally, in the process of re-mixing of records from past decades, the unprocessed tracks are not accessible. Hence, an audio effect removal system could facilitate the restoration and re-mixing of old records.

As non-linear distortion is one of the most commonly used effects for electric instruments, this work focuses on musical distortion effects that are used for aesthetic means (*e.g.*, guitar overdrive/distortion pedals) and in the process of mixing (*e.g.*, tape saturation). These distortion effects result in added harmonics, intermodulation distortion, and a compressed sound and are often classified as overdrive, distortion and fuzz: while overdrive usually refers to clipping the signal moderately, fuzz does that heavily [10].

This paper aims to investigate different deep neural network (DNN) approaches regarding their applicability to the audio effect removal problem, particularly by reviewing the special case of distortion removal. Firstly, we provide a comparative study of four different neural network architectures on the task of distortion removal in guitar signals when the clean signal is superimposed. Then, we compare the same architectures and one state-of-the-art declipping algorithm on the task of hard-clipping removal in guitar signals as well as generic music signals. For the evaluation, we review different metrics in their capabilities to assess the quality of the output of an audio effect removal system. Finally, we show that the Demucs architecture [11] surpasses one state-of-the-art method in the declipping task on a large-scale music dataset. Audio examples are available online at <https://joimort.github.io/distortionremoval/>.

This paper is organized as follows: Section II gives a formal introduction to the audio effect removal problem and introduces the types of distortions that were used throughout this study. As the removal of distortion effects is closely related to the problem of declipping, Section III briefly discusses previous work on iterative declipping algorithms and intro-

Manuscript submitted to the Journal of the Audio Engineering Society on January 24, 2022.

^{*}This work was performed while interning at Sony Europe B.V., Stuttgart, Germany.

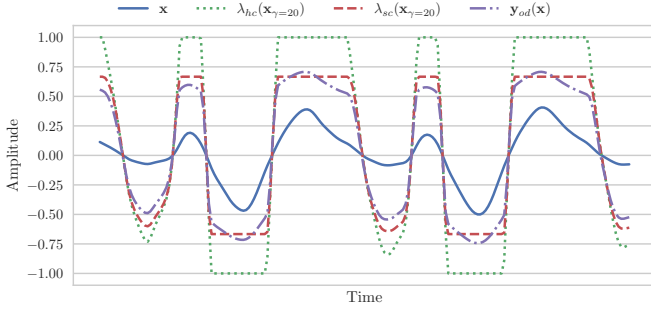


Fig. 1. Example of different distortion types applied to a guitar signal. The input signal x is amplified before being modified by a wave-shaper function.

duces previous DNN-based approaches. The methods that are investigated in this work are outlined in Section IV. Section V describes the data that were used to train the neural networks, reports details about the experimental setup, and presents the objective metrics that were chosen for evaluation. The results of the comparative study are reviewed and discussed in Section VI. Lastly, Section VII gives a conclusion and presents an outlook for future work.

II. PROBLEM SETTING

We introduce audio effect removal as the task of recovering the original discrete audio signal $\mathbf{x} \in \mathbb{R}^n$ from the processed discrete signal $\mathbf{y} \in \mathbb{R}^n$, which is obtained by applying the possibly non-linear and time-varying function f to the signal \mathbf{x} :

$$y_k = g_{\text{wet}} f(x_k, x_{k-1}, \dots, x_{k-l}; k) + g_{\text{dry}} x_k, \quad (1)$$

with k denoting the index of the time-discrete signals, g_{wet} the weight of the wet signal, and g_{dry} the weight of the dry signal.

The goal is to find an estimation $\hat{\mathbf{x}}$ of the original signal by estimating the inverse function f^{-1} :

$$\hat{x}_k = f^{-1}(y_k, y_{k-1}, \dots, y_0; k). \quad (2)$$

Generally, distortion effects clip the input signal and can be divided into systems that apply hard-clipping or soft-clipping. Figure 1 highlights the difference between these two distortion types. While hard-clipping cuts off the amplitude when it exceeds a defined threshold (typical for saturation in digital signal processing), soft-clipping gradually applies a smooth transition before reaching a fully saturated state (typical for saturation in analog amplifiers). As this work focuses on both types of distortion, we introduce the following generic formulation of a wave-shaper that maps the amplified signal $\mathbf{x}_\gamma = 10^{\frac{\gamma}{20}} \mathbf{x}$ to a fixed range:

$$\mathbf{y} = \lambda(\mathbf{x}_\gamma) \quad \text{with} \quad \lambda : \mathbb{R} \rightarrow [-\theta_c, \theta_c]. \quad (3)$$

Here, γ denotes the gain in decibels, λ the arbitrary wave-shaper function, and θ_c the fixed clipping threshold. For the case of hard-clipping, λ is defined as:

$$\lambda_{\text{hc}}(m) = \begin{cases} m, & \text{if } |m| \leq 1 \\ \text{sgn}(m) & \text{otherwise,} \end{cases} \quad (4)$$

with sgn denoting the sign function. In order to simulate a soft-clipping behavior, λ could, for example, be defined as the following function:

$$\lambda_{\text{sc}}(m) = \begin{cases} m - \frac{1}{3}m^3, & \text{if } |m| \leq 1 \\ \frac{2}{3}\text{sgn}(m) & \text{otherwise.} \end{cases} \quad (5)$$

Modeling the characteristics of analog distortion devices in reality is more complex: [2] provides an overview over different methods while discussing DNN-based approaches. In order to simplify the problem for our investigation, we focus on static wave-shaping. The overdrive algorithm of the audio editing software SoX [12] is an example of static wave-shaping and can be formulated using:

$$d_k = \lambda_{\text{sc}}(x_{\gamma,k}) - \lambda_{\text{sc}}(x_{\gamma,k-1}) + 0.995d_{k-1} \quad (6)$$

$$\mathbf{y}_{\text{od}}(\mathbf{x}, \mathbf{d}) = g_{\text{dry}}\mathbf{x} + g_{\text{wet}}\mathbf{d},$$

with \mathbf{d} being the soft-clipped signal passed through an infinite impulse response (IIR) filter with a band-pass character that filters out only very low and high frequencies. \mathbf{y}_{od} is a mixture of the output of the filter and the dry signal. The implementation uses fixed weights for mixing dry ($g_{\text{dry}} = 0.5$) and wet ($g_{\text{wet}} = 0.75$) signals.

III. RELATED WORK

To the best of our knowledge, there has been no previous research on distortion effect removal in the context of music production. Therefore, this section outlines the most relevant iterative and DNN-based declipping approaches, as declipping is a special case of distortion effect removal.

A. Iterative Declipping Methods

Previous research on declipping approaches focused mainly on unsupervised algorithms that recover the signal assuming a generic regularization such as signal sparsity [13]. Usually, these approaches target the idealized hard-clipping case only (see Eq. 3 and 4). While early approaches were based on auto-regressive models [14], today's state-of-the-art methods evolved by combining ideas from inverse problems and sparse regularization [15].

Generally, a clipped signal can be divided into samples that are reliable (indices R), samples clipped from above at the threshold θ_c (indices H), and samples clipped from below at $-\theta_c$ (indices L). Using this definitions, the clipping consistency constraint can be formulated (see Eq. 8). Incorporating this constraint at each iteration was a crucial step towards better-performing algorithms [15].

Recently, [13] and [15] discussed popular declipping algorithms. One of the current state-of-the-art methods is A-SPADE, which will serve as a baseline for this study. The algorithm is introduced in more detail in Section IV.

A different approach was proposed by [16] that is based on inverting dynamic range compression (DRC). DRC is an audio effect that generally attenuates loud sounds and amplifies quiet sounds, and hence, results in a reduction of the signal's dynamic range. It is analytically invertible when the parameters are known. A special case of DRC is the

limiter that ensures that the audio never exceeds the maximum allowed threshold and, therefore, can be regarded as clipping. The authors declip a signal by inverting the limiter based on their DRC model using the parameter estimation method from [17].

B. DNN-Based Declipping

In contrast to iterative algorithms, to date, there are only a few contributions comprising supervised DNNs.

Kashani *et al.* [18] introduced a declipping method that is based on the U-Net architecture [19]. It operates on magnitude spectrograms as input and output while the output's waveform is obtained by reusing the phase information from the distorted input signal. The system is trained and evaluated on pairs of hard-clipped and clean speech samples.

Mack and Habets [20] proposed an architecture comprising a deep filtering method that works on complex spectrogram and hence, also considers phase information. Similar to [18], they train the system on speech data only. Unlike any other approach included in this paper, they not only investigate the system on the hard-clipping case but also on the soft-clipping case.

IV. METHODS

This section describes four neural network architectures that we selected from the literature and evaluated on the distortion removal task. The evaluation covers the following models: CRAFx [21], Wave-U-Net [22], Open-Unmix [23] and Demucs [11]. The first one was designed for audio effect modeling, the others for music source separation. Additionally, we provide a brief description of our baseline for the declipping task, A-SPADE [24].

A. CRAFx

The convolutional and recurrent audio effects modeling architecture (CRAFx) was proposed as a system for modeling time-varying audio effects with a neural network [21]. The end-to-end model operates on the signal in the time domain and is divided into an adaptive front-end (encoder), a bi-directional long-short-term-memory (BLSTM)-based structure that applies the modeled effect in the latent space, and a synthesis back-end (decoder).

Firstly, the adaptive front-end performs a one-dimensional convolution, which acts as a learnable frequency decomposition. Then, a depth-wise one-dimensional convolution is used as a learnable filterbank. Next, the output is reduced using maximum pooling. A three-layer BLSTM module enables the network to learn long- and short-time dependencies, and hence, allows to model time-varying effects. The last BLSTM layer applies a smooth adaptive activation function (SAAF): previous research showed that SAAFs [25] prove beneficial in modeling non-linearities in audio processing tasks [26]. After un-pooling, a multiplicative residual connection from the output of the first convolutional layer is used to facilitate re-synthesizing the waveform. Finally, the synthesis back-end applies four fully-connected layers, models dependencies

between channels by scaling the channel-wise information and uses the transposed convolution kernel from the frequency decomposition to deconvolve the signal.

In contrast to the other neural-network-based models presented in this section, this architecture employs several strong architectural priors in the context of audio effects.

B. Open-Unmix

Open-Unmix (UMX) was introduced as a reference implementation for music source separation [23]. The architecture is based on the BLSTM model from [27] and uses magnitude spectrograms as input features.

First, a single fully-connected layer reduces the input spectrogram size to 512 output bins. Furthermore, batch normalization is applied to better handle the signals' dynamical range. The essential element of Open-Unmix is its three-layer BLSTM network that enables to learn both long and short time dependencies [28]. The size of the output of the BLSTM is again reduced by a single connected layer, normalized, and upsampled to the output dimensions. Finally, an element-wise multiplication of the input spectrograms with the estimated masks yields the final output to ensure that the network learns the ratio of the input belonging to the target source instead of the actual value.

Commonly, spectrogram-based source separation models are compared with the oracle performance of an ideal ratio mask (IRM) that is defined as the ratio between the reference and the test spectrogram [29] in decibels. For reconstruction, the phase of the input signal is used.

We include this model in our evaluation as it has relatively weak architectural priors, making it a potential candidate also for the task of audio effect removal.

C. Wave-U-Net

Wave-U-Net was proposed as one of the first end-to-end approaches for music source separation based on the time domain, and hence, incorporates not only the magnitude but also the phase of music signals [22]. It adapts the U-Net architecture [19] for one-dimensional audio signals.

The encoder-decoder architecture consists of L levels each containing a downsampling and upsampling block. A downsampling block applies a 1-D convolution and decimates the output with a factor of two. Likewise, an upsampling block applies a 1-D convolution and upsamples the output with a factor of two using linear interpolation. Hence, each level increases the number of features on coarser time scales. A concatenative skip connection between each level facilitates reconstruction.

We reduced the models' number of learnable parameters from 17 million to approximately 1 million by decreasing the number of layers, in order to cope with overfitting.

Despite the model not reaching the performance of today's source separation architectures [6], we included it in the evaluation due to its weak architectural priors.

D. Demucs

Like Wave-U-Net, Demucs was initially designed to be an end-to-end model for music source separation in the time domain [11]. While it builds on the Wave-U-Net model, it introduces several improvements to the architecture. The model comprises a convolutional encoder, a BLSTM structure, and a convolutional decoder.

Each of the encoder's L levels consists of a 1-D convolution, while the initial number of output channels doubles with each level. Each level uses ReLU activations and passes its output to an additional 1-D convolution with kernel size and stride equal to 1 which doubles the output channels. Then, a gated linear unit halves the output channels. After passing the last level, the output is fed to a 2-layer BLSTM structure in order to capture long-term dependencies. The decoder is defined as the inverse of the encoder and reduces the output channels with each layer. Skip-connections are used to allow a direct access to the input signal's phase while they facilitate gradient exchange between each encoder and decoder.

As for Wave-U-Net, we reduced the number of learnable parameters from 66 million to 1 million by decreasing the number of layers.

Even though the model is similar to Wave-U-Net, we evaluated it on the audio effect removal task because of its superior performance on music source separation.

E. Analysis Sparse Declipper

The analysis sparse declipper (A-SPADE) was introduced as a sparsity-based declipping algorithm that outperforms previous similar approaches [24].

For each time frame of the clipped signal \mathbf{y} , the algorithm approximates a solution of the following inverse problem:

$$\min_{\mathbf{x}, \mathbf{z}} \|\mathbf{z}\|_0 \text{ s.t. } \mathbf{x} \in \Gamma(\mathbf{y}) \text{ and } \|\mathcal{F}(\mathbf{x}) - \mathbf{z}\|_2 \leq \epsilon, \quad (7)$$

where \mathbf{z} denotes the unknown discrete Fourier coefficients of each time frame and \mathcal{F} denotes the Fourier transform operator. Γ is defined as the feasible space of solutions (clipping consistency constraint, see Sec. III-A) [13]:

$$\begin{aligned} \Gamma_R &= \{\tilde{\mathbf{x}} | M_R \tilde{\mathbf{x}} = M_R \mathbf{y}\}, & \Gamma_L &= \{\tilde{\mathbf{x}} | M_L \tilde{\mathbf{x}} \leq -\theta_c\}, \\ \Gamma_H &= \{\tilde{\mathbf{x}} | M_H \tilde{\mathbf{x}} \geq \theta_c\}, & \Gamma &= \Gamma_R \cap \Gamma_H \cap \Gamma_L, \end{aligned} \quad (8)$$

with M_R, M_H, M_L denoting the masking operators corresponding to the respective sets of samples R, H, L (see Sec. III-A), and $\tilde{\mathbf{x}}$ denoting an arbitrary time-domain signal.

A solution to this problem is obtained by using the alternating direction method of multipliers (ADMM) [30]. The resulting algorithm is derived and discussed in [24]. A-SPADE's complexity is mostly influenced by the analysis and synthesis operations that are carried out for each iteration and for each frame.

We included the algorithm in the evaluation of the declipping task as a baseline that achieves state-of-the-art performance [13, 15].

V. EXPERIMENTS

Our experiments focus on the following three scenarios. Firstly, we conducted experiments on guitar recordings that were processed using the overdrive algorithm introduced in Section II (CEG-OD). Then, we performed the same experiments by processing the same clean guitar recordings with hard-clipping (CEG-HC). Finally, we tested the systems on a more extensive dataset comprising not only guitar recordings (SignalTrain-HC) to evaluate their performance against popular declipping algorithms when the proposed models are trained on a larger dataset. This allowed us to investigate how the performance of the systems changes when increasing the amount and variety of data used to train them.

A. Data

The models introduced in Section IV were trained on three different datasets to assess the distortion effect removal capabilities. The audio signals from a dataset that contains data from a single instrument class (*e.g.*, electric guitar) exhibit similar signal statistics. In order to restrict statistics that need to be modeled in a first step, we chose to concentrate on dry guitar samples as target data.

Since a large-scale, polyphonic dataset from clean electric guitar sounds is, to the best of our knowledge, not available¹, we used an internal dataset, which we refer to as CEG (Clean Electric Guitar Effects) dataset. The data was gathered from various sources, mainly commercial audio loop packages and live recordings of solo guitar playing. The dry dataset has a duration of 1.68 hours. All signals were re-sampled to a sampling rate of $f_s = 16$ kHz in order to align the sampling rate of all signals.

To create the processed input dataset CEG-OD, overdrive (see Eq. 6) was applied to the data using five uniformly sampled gain levels in the range of $\gamma \in [20, 50]$ dB. Likewise, the input dataset for the hard-clipping task, CEG-HC, was created using hard-clipping (see Eq. 3 and 4) and five uniformly-sampled gain levels in the range of $\gamma \in [20, 50]$ dB, respectively. CEG-OD and CEG-HC have a total length of 8.4 hours.

Although CEG represents a good source of data for our experiments due to its specificity of instrument, it remains a limited resource in terms of size, variety and realism. Before attempting to train a system to handle recordings in real environments (*e.g.*, a commercial song), we need to investigate how the current models at our disposal handle the availability of more and diverse training data. For this purpose, we also performed experiments on the SignalTrain dataset, which consists of more than 24 hours of music and randomly-generated test sounds [32].

By applying hard-clipping to this clean data, we created SignalTrain-HC. In contrast to CEG-HC and CEG-OD, hard-clipping was applied online during training using a uniformly-sampled input SDR value in the range $\text{SDR}_{\text{inp}} \in [1, 20]$ dB.

¹It must be noted that a publicly available guitar dataset for the recognition of audio effects exists (IDMT-SMT-Audio-Effects [31]). However, the dataset contains primarily homogeneous monophonic sounds and therefore, we choose to use the CEG dataset instead.

During the evaluation stage, we applied each input SDR in the set $\text{SDR}_{\text{inp}} \in \{1, 3, 5, 7, 10, 15, 20\}$ dB to each sample in the test set. It should be noted that this procedure results in a range of hard-clipping gains that are below the gains used for CEG-HC.

Each dataset was split into subsets for training (80%), validation (10%) and test (10%). We evaluate the models on the test splits only, as they were never considered in the optimization procedure of the models.

B. Experimental Setup

We used the implementations of Demucs, Wave-U-Net, and UMX provided by the original authors, while CRAFx was implemented following the specifications in [21].

During the supervised training procedure, Adam [33] is used as optimizer with initial learning rates according to the respective original implementations. The learning rate is reduced by a factor of 10 after 150 epochs of no decrease in the validation loss. All models are optimized using the source-to-distortion ratio (see Section V-C) between their outputs and the respective targets. We stopped all trainings after 1000 epochs (in one epoch the model iterates over the whole training set). All models process audio sequences randomly extracted from each clip in the dataset; the length of the extracted sequences is equal to 2 seconds (2.3 seconds for CRAFx due to its architecture). We used a batch size of 16 for all experiments.

C. Objective Metrics

In order to assess the quality of the models, four different metrics are computed: the scale-invariant source-to-distortion ratio (SI-SDR), the perceptual evaluation of audio quality (PEAQ), the R_{nonlin} metric, and the Fréchet audio distance (FAD).

1) *Scale-Invariant Source-to-Distortion Ratio*: In speech enhancement and source separation, the ubiquitous measure to estimate the quality of a system is the source-to-distortion ratio (SDR). A recent overview study on declipping algorithms [13] used the difference of the SDR between the output and reference signal (SDR_{out}) and the SDR between the distorted and reference signal (SDR_{inp}) as evaluation metric. In order not to penalize methods that produce inconsistent outputs in the reliable, non-clipped part, they consider only clipped regions of the signal for computing the SDR.

As we used a different method to distort the signals (*i.e.*, amplifying and clipping by a wave-shaping function instead of clipping at a variable threshold), the same definition of the evaluation metric would not be applicable. For this reason, we follow the approach of [34] and use the scale-invariant SDR (SI-SDR). It is obtained by rescaling the target signal such that the residual is orthogonal to it by using the optimal scaling factor $\frac{\hat{s}^T s}{\|\hat{s}\|^2}$:

$$\text{SI-SDR} = 10 \log_{10} \left(\frac{\left\| \frac{\hat{s}^T s}{\|\hat{s}\|^2} s \right\|^2}{\left\| \frac{\hat{s}^T s}{\|\hat{s}\|^2} s - \hat{s} \right\|^2} \right), \quad (9)$$

where s denotes the clean signal and \hat{s} the reconstruction of the clean signal (in our case, the output of the model).

An evaluation exclusively based on the physical similarity of the signals (*e.g.*, by means of SI-SDR) does not necessarily imply a correlation with human perception [35, 36]. Accordingly, we observed that the SI-SDR scores occasionally disagreed with our qualitative evaluation. Therefore, we also considered three metrics based on human perception.

2) *Perceptual Evaluation of Audio Quality*: The ITU-R standard perceptual evaluation of audio quality (PEAQ) [37] is a widely used perceptual metric [13, 15, 38, 39] that measures the amount of degradation between two generic audio signals.

The model applies a fast Fourier transform (FFT)-based peripheral ear model to both the reference and the test signal in order to calculate an estimate for the audible signal components. The computation of the score relies on model output variables (MOVs) derived by a comparison of mid-level feature representations of the reference and test signal, which leads to an estimate of the audible difference per variable (*e.g.*, modulation difference, audible linear distortion, signal bandwidth). The MOVs are then fed to a neural network which maps these mid-level features to a single score value. Finally, the network outputs an Overall Difference Grade (ODG), which can reach values between 0 (*imperceptible impairment*) and -4 (*very annoying impairment*).

3) *Perceived Quality of Non-linearly Distorted Music and Speech Signals*: Even though PEAQ is used in declipping and audio restoration studies [13, 15, 38], it was initially developed for bit-rate reduction systems. Therefore, we additionally evaluated the models with the R_{nonlin} metric, which was developed specifically for non-linear distortions [40] and, like PEAQ, takes into account the human auditory system.

Firstly, the reference and test signals are split into frames and filtered for outer- and middle ear correction by using a finite impulse response (FIR) filter. Both signals are fed to a filterbank of 40 1-ERB_N-wide gammatone filters, which model the human auditory filters. The maximum value of the short-term cross-correlation between the reference and test signal is computed for each output, which allows for minor frequency-dependent time delays. This value ideally describes the number of frequency components which are not present in the reference signal for each filter.

Next, the output is weighted according to the present energy in each filter output, and is finally accumulated for each frame and then averaged across frames. R_{nonlin} is defined between 0 (*high distortion*) and 1 (*no distortion*).

4) *Fréchet Audio Distance*: The Fréchet audio distance (FAD) was recently proposed as a reference-free evaluation metric for music enhancement algorithms. It is shown to correlate more with human perception than the SDR [41].

In order to obtain the FAD, the embedding statistics of both the whole clean and distorted test set are generated using a VGGish model [42]. Then, two multivariate Gaussians are computed from both the test embeddings and the reference embeddings. Finally, the FAD is calculated based on the Fréchet distance between these Gaussians [43]. The VGGish model that is employed to obtain the embedding for each sample uses mel spectrograms as its input. However, the authors verified that the FAD could still be beneficial in recognizing phase distortions.

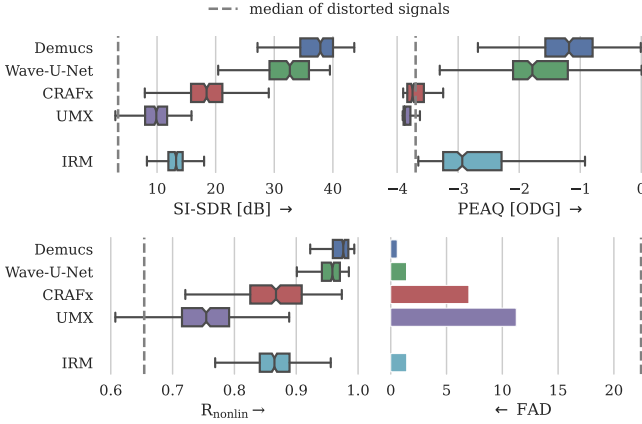


Fig. 2. Box plot of scores for the CEG-OD dataset that was augmented using the overdrive algorithm. The boxes show the first and third quartile of the data while the median is indicated with a line in the box. Higher score indicates superior performance except for FAD. Demucs can be regarded as the best model for all metrics. The results indicate that time-domain-based models are better suited to solve the task of overdrive removal.

VI. RESULTS

In this section, we provide the results of the experiments introduced in the previous section.

A. De-overdrive (CEG-OD)

Figure 2 shows the results of the models that remove overdrive from guitar tracks. The scores are computed on the test subset of our CEG-OD dataset.

Firstly, in SI-SDR, both Demucs and Wave-U-Net perform exceptionally well and even outperform the ideal-ratio-mask by more than 24 dB. While CRAFx yields considerably worse performance, it also surpasses the IRM oracle. UMX is the least performing of all the models in our comparison. It should be noted that for UMX, a model that operates on magnitude spectrograms, the IRM represents its upper limit in performance.

Similar results are obtained with PEAQ, R_{nonlin} and FAD: while Demucs and Wave-U-Net yield the best scores and surpass the IRM, the ones for CRAFx and UMX are considerably worse.

Overall, Demucs can be regarded as the best model regarding all metrics. Our scores suggest that time-domain-based models are better suited to solve the task of overdrive removal.

B. Declipping (CEG-HC)

Figure 3 shows the results on the task of declipping on guitar recordings. Generally, we experienced a drop in the scores: now the models have been trained on a different distortion method (hard-clipping), which appears to be an ill-posed problem. Additionally, we report scores for our declipping baseline, A-SPADE, introduced in Section IV.

Despite the general performance drop, Demucs surpasses the results of A-SPADE in terms of SI-SDR by almost 1 dB. Nevertheless, none of the models surpasses the IRM oracle. While UMX and Wave-U-Net yield a similar performance, CRAFx is the method with lowest scores.

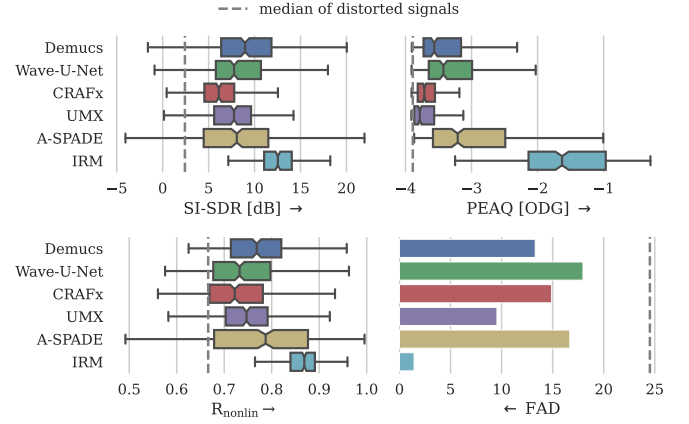


Fig. 3. Box plot of scores for the CEG-HC dataset that was augmented using the hard-clipping algorithm. The boxes show the first and third quartile of the data while the median is indicated with a line in the box. Higher score indicates superior performance except for FAD. It is difficult to clearly determine the best model, although Demucs represents a good compromise for all the metrics.

Regarding PEAQ, no method surpasses the IRM and the A-SPADE algorithm. As before, Demucs and Wave-U-Net have similar performance: while PEAQ slightly favors the latter, SI-SDR favors the former. In contrast to the previous results, CRAFx has no significant advantage over UMX.

While Demucs achieves the best score for R_{nonlin} among the neural models, it does not surpass A-SPADE (the difference in their score is marginal). Interestingly, UMX achieves better results than CRAFx and Wave-U-Net. As the R_{nonlin} metric was explicitly designed to detect non-linear distortions, we conclude that UMX' outputs contain fewer non-linear distortions than the outputs of CRAFx and Wave-U-Net.

Surprisingly, when computing FAD, UMX outperforms all other methods, including A-SPADE. This might be accounted to the fact that the FAD is based on the mel spectrum, whereas UMX optimizes the magnitude spectrogram. While Demucs and CRAFx outperform A-SPADE in FAD as well, Wave-U-Net's score is slightly worse. The FAD for the IRM is relatively small because the difference between the reference and test embeddings from the VGGish model can be traced back to the masking operation and quantization.

In contrast to the de-overdrive task, it is difficult to determine the best model. However, Demucs constitutes a good compromise regarding performance since it yields first- or second-best results for all metrics.

C. Declipping (SignalTrain-HC)

Figure 4 shows the results for declipping SignalTrain-HC. Due to the lower gains that are used to prepare the data (see Section V-A), the overall performance seems to be superior but cannot be directly compared to the previous results. Because of its considerably worse performance in the previous task, CRAFx was left out of the evaluation.

Demucs surpasses all other models in SI-SDR, including IRM and A-SPADE. Moreover, Wave-U-Net and UMX both surpass A-SPADE, but not the IRM (although nearly reaching it).

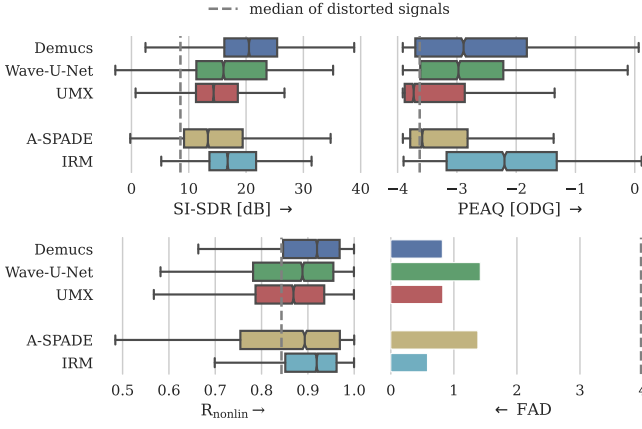


Fig. 4. Box plot of scores for the SignalTrain-HC dataset that was augmented using the hard-clipping algorithm. The boxes show the first and third quartile of the data while the median is indicated with a line in the box. Higher score indicates superior performance except for FAD. Demucs can be regarded as the best model regarding the median score across all metrics.

PEAQ gives a similar ranking of the methods: only UMX cannot reach the A-SPADE baseline. None of the neural methods surpasses the IRM. In terms of R_{nonlin} , the same ranking is achieved again, with Demucs surpassing, Wave-U-Net reaching, and UMX just missing A-SPADE.

FAD highlights that UMX (frequency-domain model) and Demucs (time-domain model) achieve comparable performance, outperforming the baseline, but not surpassing the IRM.

Only by looking at SI-SDR or PEAQ we notice the superiority of the time-domain models. Future research should investigate whether the waveform in the time domain is the best input representation for the task, compared to e.g., the real and imaginary part of a spectrogram (*cf.* [44]), or both the waveform and the spectrogram (*cf.* [45]).

Ultimately, Demucs can be considered to be the best model in our experiments for the task of declipping on SignalTrain.

Dependency on Input SDR: In order to investigate the performance of the models as a function of the amount of distortion present in the input signal, Figure 5 shows the scores for SI-SDR, PEAQ, and R_{nonlin} for varying SDR_{inp} .

The results suggest that the relationship between SDR_{inp} and SI-SDR is approximately linear. A-SPADE is the only exception, since for low SDR_{inp} values (*i.e.*, for highly distorted inputs) the performance drops significantly (left side of Figure 5). This performance decrease has been reported previously in the literature for various declipping algorithms [13, 15]. At the same time, we see all models decrease the SI-SDR improvement for high SDR_{inp} (*i.e.*, right side of Figure 5): since the input signal presents low distortion, there is also less margin for improvement.

We observe a non-linear relationship between SDR_{inp} and PEAQ, as the curve’s slope increases with higher SDR_{inp} . This is due to PEAQ not being able to distinguish clearly signals with large impairment, as already observed by [46].

Furthermore, we notice a non-linear relationship between

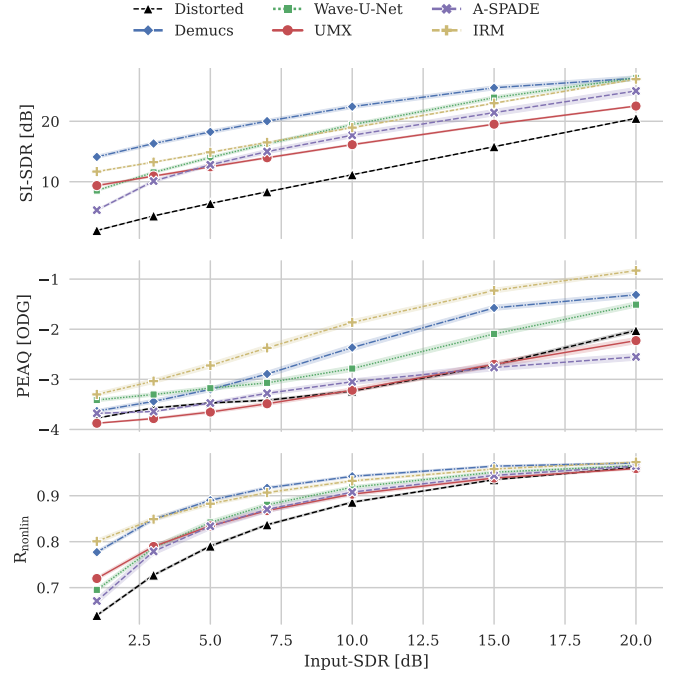


Fig. 5. Mean scores obtained from the SignalTrain-HC dataset in comparison with the input SDR. The 95 % confidence interval is depicted with a light colored area around each line. Additionally, the black, dashed line depicts the respective score for the distorted input signals. A-SPADE’s performance drops significantly towards heavily clipped signals with a SDR_{inp} of 1 dB; the neural models do not exhibit such a behavior.

R_{nonlin} and SDR_{inp} , which resembles a logarithmic behavior. R_{nonlin} does not saturate for high distortion, which makes it a good candidate for the comparison of significantly clipped signals. However, it does saturate for low distortions, therefore cannot be used reliably when the input signal is only slightly clipped.

D. Discussion

Qualitative Evaluation: Although the abundance of evaluation metrics in the literature has the potential to analyze the results in very detailed ways, it does not always aid the judgement of which method is best in which context. Often, different applications have different requirements on the sound quality and can afford some types of distortions or artifacts to be left in the signal. We, therefore, report here some qualitative considerations about our results, with the aim of finding some descriptive patterns among them. Figure 6 shows spectrograms of a hard-clipped guitar signal and the corresponding outputs of all models under evaluation.

One first remark is that the characteristics of the artifacts that each model produces are consistent, independently on the task it is applied to. This suggests that the architectural features of the models are the aspect that is responsible the most for the characteristics of the artifacts that are produced. Nevertheless, for the time-domain-based models, artifacts are less prominent in the de-overdrive task. Here, Demucs often produces outputs that are virtually indistinguishable from the original signal.

Generally, Demucs is the model that most often produces high quality results. Especially for inputs with low amount

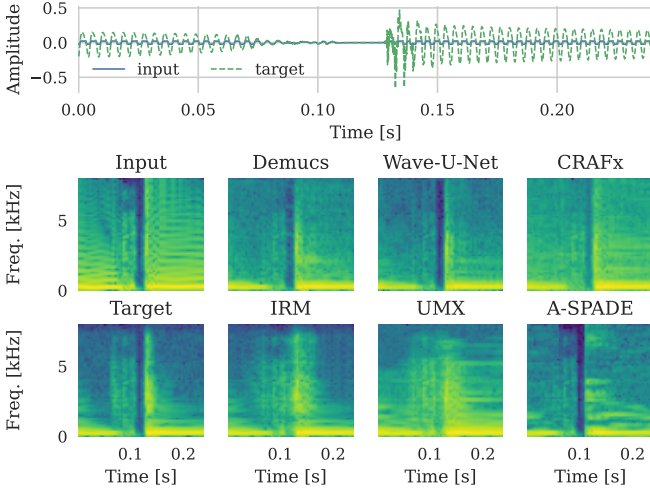


Fig. 6. Spectrograms of a hard-clipped guitar input signal, its target signal, and the output of each method. The respective time-domain input and target signal is shown at the top (the hard-clipped signal was re-scaled so that it overlaps with the target signal in the reliable part). While all methods reduce the harmonics in the clipped signal, it can be observed that IRM and UMX smear the transients. A-SPADE relies on the strongest bins in the clipped spectrum which leads to tonal artifacts.

of distortion, it can reconstruct the original sound without any perceptual artifact. When this is not the case, part of the distortion characteristics of the input can be heard in the output, especially for signals with low amplitude. Wave-U-Net behaves very much like Demucs, although it often struggles to reach the same quality.

UMX generally manages to remove the distortion characteristics very well. Unfortunately, this comes at the cost of strong phasing artifacts: despite the absence of the input distortions, the spectral features of the output are not necessarily consistent with the ones of the target. This is most likely due to the fact that UMX uses the phase of the distorted input to reconstruct the signal in the time domain. We experience the same behavior with the IRM (which achieves better quality): this is an additional clue that the phasing artifacts are to be attributed to UMX operating in the frequency domain only. Moreover, Figure 6 highlights that the transients are smeared by re-using the phase of the degraded signal.

CRAFX does not suffer from phasing artifacts, but occasionally leaves part of the distortion features in the output. In some cases, the model fails to reconstruct the onset of some notes, penalizing the listening experience.

Finally, A-SPADE is the model that exhibits the strongest and most frequent artifacts, especially for strongly clipped signals. Although it considers phase information by working in the complex frequency domain, its iterative nature (that relies on the strongest frequency bins) leads to non-optimal solutions. Potentially, these artifacts result from enhancing overtones that can not be found in the original signal (see Fig. 6). Nevertheless, distortion features (like those left by Demucs) or transient smearing (left by UMX) do not occur.

Influence of the Dry Signal: We have observed a substantial difference in performance between models that need to remove overdrive (CEG-OD dataset) and models that need

to remove hard-clipping (CEG-HC dataset). The superior performance of the models trained and tested on CEG-OD can be mainly traced back to the presence of the non-distorted signal in the overdrive output and not to the soft-clipping character of the specific overdrive implementation. We verified this hypothesis with a side experiment: when training Wave-U-Net on hard-clipped data superimposed with the clean signal (even when the amplitude of the clean signal is considerably low), we obtain results similar to those in the de-overdrive task (median results without superposition: SI-SDR = 7.2 dB, with superposition: SI-SDR = 34.4 dB). While the performance drop is present for all metrics, it is less pronounced for UMX which seem to not utilize the additional information in the signal.

Many audio effects used in music production blend the processed, wet sound with the original, dry sound: the fact that the models under evaluation perform better when the dry signal is blended with the wet signal suggests that the methods we analyzed can potentially be used in the removal of any audio effect that employs wet/dry mixing.

Inference Speed: The benefits of Demucs in the context of declipping go beyond the quality of its outputs: using a neural approach has also advantages in inference speed. Inference with A-SPADE (currently one of the best performing algorithms in the literature) is comparably slow (real-time factor $\times RT \in [4.2, 27.3]$ dep. on SDR_{inp} [15]), being an iterative approach that requires a computation of the Fourier transform and its inverse at each iteration. Demucs ($\times RT = 0.072$), Wave-U-Net ($\times RT = 0.113$) and UMX ($\times RT = 0.026$) instead, allow for fast inference, even surpassing real-time constraints independently on SDR_{inp} , without sacrificing the quality of the results.

Generalization: While neural networks offer improvements in quality and inference speed, they suffer from potentially poor generalization: in our experiments we significantly reduced the number of learnable parameters in all models, possibly affecting how well they can handle a wide variety of input signals.

During our experiments, the systems under evaluation showed a sufficient degree of generalization over unseen audio signals when processed using the same distortion algorithms. Nevertheless, their performance drops significantly when processing real-world distorted guitar sounds, as we limited our experiments to two simplified methods for distortion, which represent only part of a commercial distortion effect. The positive outcomes of our experiments suggest that the neural models in this work can potentially be used to remove more complex distortion effects, if the training data includes such complex distortion algorithms (or their high-quality emulation, e.g., by using the frameworks [47] or [48]). We plan to validate this hypothesis in future work.

Evaluation Metrics: The results highlight how our evaluation metrics focus on different aspects of the signals under analysis: while SI-SDR measures differences between two audio signals in the time domain, PEAQ focuses on the overall perceptual quality without differentiating between degradation related to non-linear distortions and artifacts/quality. In contrast, R_{nonlin} specifically highlights non-linear distortions that

TABLE I. Kendall correlation coefficients computed from all scores obtained in this study. FAD is not included as there is only one global value for each dataset and method. The scores of SI-SDR, PEAQ and R_{nonlin} are hardly correlated which highlights that they measure different aspects of the reconstruction quality.

	SI-SDR	PEAQ	R_{nonlin}
SI-SDR	1.00	0.37	0.53
PEAQ	0.37	1.00	0.56
R_{nonlin}	0.53	0.56	1.00

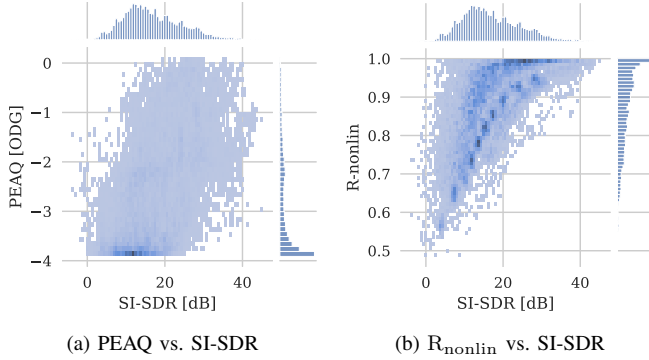


Fig. 7. Histogram plot of the PEAQ and R-nonlin scores in comparison with the SI-SDR scores for all datasets and methods.

have not been removed. Finally, FAD focuses primarily on degradation that is observable in the mel spectrum.

To further motivate the choice of the four evaluation metrics in this work, Table I shows the Kendall correlation coefficient [49] computed for each pair of metrics. We observe that all pairs of metrics have low correlation, suggesting that every metric highlights and evaluates a different aspect of the quality of the results. Since the FAD is calculated globally for the whole test and reference dataset (see Sec. V-C), its correlation values can not be computed.

Figure 7 shows histogram plots of the PEAQ and R_{nonlin} scores against the SI-SDR ones. For PEAQ, the plot further highlights the saturating behaviour towards strong clipping as a large proportion of values can be found at the negative limit of the ODG scale. Similarly, for R_{nonlin} , the plot substantiates the logarithmic relation to the SI-SDR, as well as the problem of not differentiating clearly between slightly clipped signals.

VII. CONCLUSION

In this paper, we presented an overview of distortion effect removal while conducting a comparative study on the performance of four different supervised deep learning approaches on the task. We found that Demucs achieves high quality according to the evaluation metrics, especially when the distortion algorithm to be removed blends the distorted sound with the original one. This highlights the potential of the proposed approach for other audio effects that mix the dry and wet signals (e.g., parallel compression, reverberation, delay, modulation effects).

Moreover, we showed that Demucs, Wave-U-Net, and UMX outperform one state-of-the-art declipping method on our test data. This outcome is promising, considering that the number of learnable parameters in the models were drastically reduced

with respect to their original specifications and that the dataset size to train such a system is potentially much larger than the size of the dataset we used.

By discussing the results, we stressed the usefulness of multiple evaluation metrics suitable to assess distortion removal systems. It remains an issue for future work to conduct a comparative listening test on distorted audio signals to obtain knowledge on the respective correlation between the metrics used in this study and human perception.

Future work should include gathering more clean electric guitar data and generating a dataset using high-quality distortion emulations, which is required to improve generalization on real-world data. Furthermore, the knowledge from sparsity-based declipping algorithms could yield a useful prior for declipping using DNNs.

REFERENCES

- [1] U. Zölzer, *DAFX: digital audio effects*. Chichester, West Sussex, England: Wiley, 2nd ed ed., 2011.
- [2] M. A. Martínez Ramírez, E. Benetos, and J. Reiss, “Deep Learning for Black-Box Modeling of Audio Effects,” *Applied Sciences*, vol. 10, p. 638, Jan. 2020. <http://doi.org/10.3390/app10020638>.
- [3] R. Stables, B. De Man, and J. D. Reiss, “Ten years of automatic mixing,” in *Proceedings of the 3rd Workshop on Intelligent Music Production, Salford, UK, 15 September 2017*, 2017.
- [4] M. A. Martínez Ramírez, D. Stoller, and D. Moffat, “A Deep Learning Approach to Intelligent Drum Mixing With the Wave-U-Net,” *Journal of the Audio Engineering Society*, vol. 69, pp. 142–151, Mar. 2021.
- [5] C. J. Steinmetz, J. Pons, S. Pascual, and J. Serra, “Automatic Multitrack Mixing With A Differentiable Mixing Console Of Neural Audio Effects,” in *ICASSP 2021 - 2021 IEEE International Conference on Acoustics, Speech and Signal Processing (ICASSP)*, (Toronto, ON, Canada), pp. 71–75, IEEE, June 2021. <http://doi.org/10.1109/ICASSP39728.2021.9414364>.
- [6] Y. Mitsufuji, G. Fabbro, S. Uhlich, and F.-R. Stöter, “Music Demixing Challenge 2021,” *Frontiers in Signal Processing*, vol. 1, 2022. <https://doi.org/10.3389/frsip.2021.808395>.
- [7] W. Choi, M. Kim, M. A. Martínez Ramírez, J. Chung, and S. Jung, “AMSS-Net: Audio Manipulation on User-Specified Sources with Textual Queries,” in *Proceedings of the 29th ACM International Conference on Multimedia*, pp. 1775–1783, Apr. 2021. <https://doi.org/10.1145/3474085.3475323>.
- [8] Z. Rafii, A. Liutkus, F.-R. Stöter, S. I. Mimilakis, and R. Bitner, “The MUSDB18 corpus for music separation,” Dec. 2017. <https://doi.org/10.5281/zenodo.1117372>.
- [9] D. Ronan, D. Moffat, H. Gunes, and J. D. Reiss, “Automatoic Subgrouping of Multitrack Audio,” in *Proc. of the 18th Int. Conference on Digital Audio Effects (DAFx-15)*, (Trondheim, Norway), 2015.
- [10] T. Wilmering, D. Moffat, A. Milo, and M. B. Sandler, “A History of Audio Effects,” *Applied Sciences*, vol. 10, p. 791, Jan. 2020. <http://doi.org/10.3390/app10030791>.
- [11] A. Défossez, N. Usunier, L. Bottou, and F. Bach, “Music Source Separation in the Waveform Domain,” *arXiv:1911.13254 [cs, eess, stat]*, Apr. 2021.
- [12] C. Bagwell, et al., “Sound eXchange (SoX),” Feb. 2015. <http://sox.sourceforge.net/>.
- [13] P. Závřiska, P. Rajmic, A. Ozerov, and L. Rencker, “A Survey and an Extensive Evaluation of Popular Audio Declipping Methods,” *IEEE Journal of Selected Topics in Signal Processing*, vol. 15, pp. 5–24, Jan. 2021. <http://doi.org/10.1109/JSTSP.2020.3042071>.
- [14] A. Janssen, R. Veldhuis, and L. Vries, “Adaptive interpolation of discrete-time signals that can be modeled as autoregressive processes,” *IEEE Transactions on Acoustics, Speech, and Signal Processing*, vol. 34, pp. 317–330, Apr. 1986. <http://doi.org/10.1109/TASSP.1986.1164824>.
- [15] C. Gaultier, S. Kitić, R. Gribonval, and N. Bertin, “Sparsity-Based Audio Declipping Methods: Selected Overview, New Algorithms, and Large-Scale Evaluation,” *IEEE/ACM Transactions on Audio, Speech, and Language Processing*, vol. 29, pp. 1174–1187, 2021. <http://doi.org/10.1109/TASLP.2021.3059264>.

- [16] S. Gorlow, J. D. Reiss, and E. Duru, "Restoring the dynamics of clipped audio material by inversion of dynamic range compression," in *2014 IEEE International Symposium on Broadband Multimedia Systems and Broadcasting*, (Beijing, China), pp. 1–5, IEEE, June 2014. <http://doi.org/10.1109/BMSB.2014.6873575>.
- [17] S. Gorlow and J. D. Reiss, "Model-Based Inversion of Dynamic Range Compression," *IEEE Transactions on Audio, Speech, and Language Processing*, vol. 21, no. 7, pp. 1434–1444, 2013. <http://doi.org/10.1109/TASL.2013.2253099>.
- [18] H. B. Kashani, M. M. Goodarzi, A. Jodeiri, and S. G. Firooz, "Image to Image Translation based on Convolutional Neural Network Approach for Speech Decipping," *4th Conference on Technology In Electrical and Computer Engineering (ETECH 2019)*, 2019.
- [19] O. Ronneberger, P. Fischer, and T. Brox, "U-Net: Convolutional Networks for Biomedical Image Segmentation," in *Medical Image Computing and Computer-Assisted Intervention – MICCAI 2015* (N. Navab, J. Hornegger, W. M. Wells, and A. F. Frangi, eds.), (Cham), pp. 234–241, Springer International Publishing, 2015.
- [20] W. Mack and E. A. P. Habets, "Decipping Speech Using Deep Filtering," in *2019 IEEE Workshop on Applications of Signal Processing to Audio and Acoustics (WASPAA)*, pp. 200–204, Oct. 2019. <http://doi.org/10.1109/WASPAA.2019.8937287>.
- [21] M. A. Martínez Ramírez, E. Benetos, and J. D. Reiss, "A general-purpose deep learning approach to model time-varying audio effects," in *22nd International Conference on Digital Audio Effects (DAFx-19)*, June 2019. arXiv: 1905.06148.
- [22] D. Stoller, S. Ewert, and S. Dixon, "Wave-U-Net: A Multi-Scale Neural Network for End-to-End Audio Source Separation," in *Proceedings of the 19th ISMIR Conference, Paris, France, September 23-27, 2018*, (Paris), June 2018.
- [23] F.-R. Stöter, S. Uhlich, A. Liutkus, and Y. Mitsufuji, "Open-Unmix - A Reference Implementation for Music Source Separation," *Journal of Open Source Software*, vol. 4, p. 1667, Sept. 2019. <http://doi.org/10.21105/joss.01667>.
- [24] S. Kitić, N. Bertin, and R. Gribonval, "Sparsity and Cosparsity for Audio Decipping: A Flexible Non-convex Approach," in *Latent Variable Analysis and Signal Separation* (E. Vincent, A. Yeredor, Z. Koldovský, and P. Tichavský, eds.), (Cham), pp. 243–250, Springer International Publishing, 2015. https://doi.org/10.1007/978-3-319-22482-4_28.
- [25] L. Hou, D. Samaras, T. M. Kurc, Y. Gao, and J. H. Saltz, "ConvNets with Smooth Adaptive Activation Functions for Regression," *Proceedings of the 20th International Conference on Artificial Intelligence and Statistics (AISTATS) 2017*, 2017.
- [26] M. A. Martínez Ramírez and J. D. Reiss, "Modeling Nonlinear Audio Effects with End-to-end Deep Neural Networks," in *ICASSP 2019 - 2019 IEEE International Conference on Acoustics, Speech and Signal Processing (ICASSP)*, (Brighton, United Kingdom), pp. 171–175, IEEE, May 2019. <http://doi.org/10.1109/ICASSP.2019.8683529>.
- [27] S. Uhlich, M. Porcu, F. Giron, M. Enenkl, T. Kemp, N. Takahashi, and Y. Mitsufuji, "Improving music source separation based on deep neural networks through data augmentation and network blending," in *2017 IEEE International Conference on Acoustics, Speech and Signal Processing (ICASSP)*, (New Orleans, LA), pp. 261–265, IEEE, Mar. 2017. <http://doi.org/10.1109/ICASSP.2017.7952158>.
- [28] S. Hochreiter and J. Schmidhuber, "Long Short-Term Memory," *Neural Computation*, vol. 9, pp. 1735–1780, Nov. 1997. <https://doi.org/10.1162/neco.1997.9.8.1735>.
- [29] A. Narayanan and D. Wang, "Ideal ratio mask estimation using deep neural networks for robust speech recognition," in *2013 IEEE International Conference on Acoustics, Speech and Signal Processing*, pp. 7092–7096, 2013. <http://doi.org/10.1109/ICASSP.2013.6639038>.
- [30] D. Gabay and B. Mercier, "A dual algorithm for the solution of nonlinear variational problems via finite element approximation," *Computers & Mathematics with Applications*, vol. 2, no. 1, pp. 17–40, 1976. [http://doi.org/10.1016/0898-1221\(76\)90003-1](http://doi.org/10.1016/0898-1221(76)90003-1).
- [31] M. Stein, J. Abeßer, C. Dittmar, and G. Schuller, "Automatic Detection of Audio Effects in Guitar and Bass Recordings," in *AES 128th Convention*, (London, UK), May 2010.
- [32] S. H. Hawley, B. Colburn, and S. I. Mimitakis, "SignalTrain: Profiling Audio Compressors with Deep Neural Networks," in *AES 147th Convention*, May 2019.
- [33] D. P. Kingma and J. Ba, "Adam: A Method for Stochastic Optimization," in *3rd International Conference on Learning Representations, {ICLR} 2015, San Diego, CA, USA, May 7-9, 2015, Conference Track Proceedings*, 2015.
- [34] J. L. Roux, S. Wisdom, H. Erdogan, and J. R. Hershey, "SDR – Half-baked or Well Done?," in *ICASSP 2019 - 2019 IEEE International Conference on Acoustics, Speech and Signal Processing (ICASSP)*, (Brighton, United Kingdom), pp. 626–630, IEEE, May 2019. <http://doi.org/10.1109/ICASSP.2019.8683855>.
- [35] E. Cano, D. FitzGerald, and K. Brandenburg, "Evaluation of quality of sound source separation algorithms: Human perception vs quantitative metrics," in *2016 24th European Signal Processing Conference (EUSIPCO)*, (Budapest, Hungary), pp. 1758–1762, IEEE, Aug. 2016. <http://doi.org/10.1109/EUSIPCO.2016.7760550>.
- [36] V. Emiya, E. Vincent, N. Harlander, and V. Hohmann, "Subjective and Objective Quality Assessment of Audio Source Separation," *IEEE Transactions on Audio, Speech, and Language Processing*, vol. 19, pp. 2046–2057, Sept. 2011. <http://doi.org/10.1109/TASL.2011.2109381>.
- [37] T. Thiede, W. C. Treurniet, R. Bitto, C. Schmidmer, T. Sporer, J. G. Beerends, and C. Colomes, "PEAQ - The ITU Standard for Objective Measurement of Perceived Audio Quality," *Journal of the Audio Engineering Society*, vol. 48, pp. 3 EP – 29, Feb. 2000.
- [38] S. Lattner and J. Nistal, "Stochastic Restoration of Heavily Compressed Musical Audio Using Generative Adversarial Networks," *Electronics*, vol. 10, p. 1349, June 2021. <http://doi.org/10.3390/electronics10111349>.
- [39] J. You, U. Reiter, M. M. Hannuksela, M. Gabbouj, and A. Perkis, "Perceptual-based quality assessment for audio-visual services: A survey," *Signal Processing: Image Communication*, vol. 25, pp. 482–501, Aug. 2010. <http://doi.org/10.1016/j.image.2010.02.002>.
- [40] C.-T. Tan, B. C. J. Moore, N. Zacharov, and V.-V. Mattila, "Predicting the Perceived Quality of Nonlinearly Distorted Music and Speech Signals," *Journal of the Audio Engineering Society*, vol. 52, pp. 699–711, July 2004.
- [41] K. Kilgour, M. Zuluaga, D. Roblek, and M. Sharifi, "Fréchet Audio Distance: A Reference-Free Metric for Evaluating Music Enhancement Algorithms," in *Interspeech 2019*, pp. 2350–2354, ISCA, Sept. 2019. <http://doi.org/10.21437/Interspeech.2019-2219>.
- [42] S. Hershey, S. Chaudhuri, D. P. W. Ellis, J. F. Gemmeke, A. Jansen, R. C. Moore, M. Plakal, D. Platt, R. A. Saurous, B. Seybold, M. Slaney, R. J. Weiss, and K. Wilson, "CNN Architectures for Large-Scale Audio Classification," *International Conference on Acoustics, Speech and Signal Processing (ICASSP)*, Jan. 2017.
- [43] D. Dowson and B. Landau, "The Fréchet distance between multivariate normal distributions," *Journal of multivariate analysis*, vol. 12, no. 3, pp. 450–455, 1982.
- [44] W. Choi, M. Kim, J. Chung, D. Lee, and S. Jung, "Investigating U-Nets with various Intermediate Blocks for Spectrogram-based Singing Voice Separation," in *Proceedings of the 21th International Society for Music Information Retrieval Conference*, Oct. 2020.
- [45] A. Défossez, "Hybrid Spectrogram and Waveform Source Separation," in *Proceedings of the ISMIR 2021 Workshop on Music Source Separation*, Nov. 2021.
- [46] C. Creusere, K. Kallakuri, and R. Vanam, "An Objective Metric of Human Subjective Audio Quality Optimized for a Wide Range of Audio Fidelities," *IEEE Transactions on Audio, Speech, and Language Processing*, vol. 16, pp. 129–136, Jan. 2008. <http://doi.org/10.1109/TASL.2007.907571>.
- [47] M. A. Martínez Ramírez, O. Wang, P. Smaragdis, and N. J. Bryan, "Differentiable Signal Processing With Black-Box Audio Effects," in *ICASSP 2021 - 2021 IEEE International Conference on Acoustics, Speech and Signal Processing (ICASSP)*, (Toronto, ON, Canada), pp. 66–70, IEEE, June 2021.
- [48] P. Sobot, "pedalboard V0.3.10," 2021. Spotify AB, <https://github.com/spotify/pedalboard>.
- [49] M. G. Kendall, "A New Measure of Rank Correlation," *Biometrika*, vol. 30, p. 81, June 1938. <https://doi.org/10.2307/2332226>.